

Operational Space Inertia for Robots with Internal Loops

Abhinandan Jain¹

¹ Jet Propulsion Laboratory, California Institute of Technology, 4800 Oak Grove Drive, Pasadena, CA, 91109 USA,
Abhi.Jain@jpl.nasa.gov

Abstract

Operational space modeling and control are important techniques for robot manipulation. A key element of operational space control is the *operational space inertia matrix (OSIM)*. The OSIM matrix represents a mapping between end-effector spatial forces and spatial accelerations. In the case of multiple end-effectors, the OSIM also encapsulates the dynamics cross-coupling between the end-effectors. The OSIM matrix is configuration dependent. The rich structure of the OSIM for tree systems has been exploited by researchers for analysis and the development of low order computational algorithms. Extending such techniques to the OSIM for closed-chain robotic systems is the focus of this short paper. We derive explicit analytical expressions for the closed-chain OSIM that reveals its close relationship to an extended tree-system OSIM.

Keywords: *robotics, multibody dynamics*

1 Introduction

Operational space control has emerged as an increasingly important approach for the modeling and control of multi-link robotic systems [1, 2]. Operational space control focuses on the dynamical behavior of the system reflected to the task (end-effector) space during interactions with the task objects and the environment [2–6]. For humanoid systems, such interaction can involve arm end-effectors, while feet serve as the end-effectors for legged systems. The set of end-effector nodes define the operational space of the system. The control problem requires managing the motion state as well as the force interactions of the robotic system with task objects and the environment.

The advantage of the operational space control approach over joint space control is that the control problem is posed directly in terms of task space variables. Analogous to the joint space mass matrix which defines the relationship between the joint space accelerations and torques, the *operational space inertia matrix (OSIM)* defines the mapping between end-effector spatial accelerations and spatial forces. Unlike the joint-space mass matrix which is always well defined and non-singular for serial and tree systems, the OSIM may not exist. In contrast, its inverse, referred to as the *operational space compliance matrix (OSCM)* is always well-defined.

An issue for operational space control has been the significant analytical and computational complexity of the OSCM. The OSCM is defined in terms of the mass matrix inverse and can be complex and expensive to evaluate. However, such hurdles have been addressed and the rich analytical structure of the OSCM is well understood for serial [7–9] and tree-topology robotic systems [10–13]. These analytical insights have led to the development of recursive computational algorithms for serial and tree OSCM that avoid the explicit need for the mass matrix inverse. These algorithms reduce the computational cost from cubic to a linear function of the number of degrees of freedom in the system.

Several researchers have explored the generalization of operational space control and the OSCM to closed-chain systems. Closed-chain topology in robotics systems can arise from structural elements such as four-bar linkages, during coordinated multi-arm manipulation task execution, during multi-finger grasping, from ground interactions of wheeled and legged mobile platforms etc. The additional constraints restrict the allowable motion for the system. The joint space system mass matrix is singular for these systems and thus the tree OSCM concept and computational techniques do not directly extend to closed-chain topologies. Reference [14] describes an extension by projecting the joint space dynamics to a set of independent coordinates. As observed in reference [15], the disadvantage of the projected dynamics is its added additional complexity and the loss of the natural structure of the OSCM that is important for control. This reference instead exploits the parallels between the structure of the closed-chain dynamics and operational space dynamics to handle systems with general holonomic constraints. Closed-chain operational space control has also have been applied to systems with contact constraints [16] and for full-body control of humanoid robots [17].

The main contribution of this paper is in establishing the close relationship between the closed-chain OSCM and an extended OSCM for a related tree system. This connection opens the door for the application of analytical insights and

computational techniques for tree systems to closed-chain OSCM. We also develop analytical concepts and mathematical expressions for the closed-chain OSCM and the necessary conditions for its positive definiteness and the existence of the OSIM. The paper is organized as follows. Section 2 introduces the OSIM and OSCM for tree topology systems. In Section 3 we describe the dynamics of closed-chain robotic systems. Section 4 extends the notion of OSCM to closed-chain systems and develops analytical expressions for it. In Section 5 we specialize to the important case where the closure constraints are loop constraints, and show that the closed-chain OSCM is closely related to the OSCM for a related tree system.

2 Tree-Topology OSIM

Consider a tree-topology robotic system with n links and \mathcal{N} degrees of freedom, where the bodies are connected to each other via hinges. The number of such end-effector nodes is denoted n_e . The operational (or task) space of a system is defined by the configuration of the end-effector nodes on the system. Let $\mathcal{V}_e \in \mathcal{R}^{6n_e}$ denote the stacked vector of 6-dimensional spatial velocities of all the n_e end-effector nodes. The relationship between \mathcal{V}_e and the $\dot{\theta} \in \mathcal{R}^{\mathcal{N}}$ stacked vector of joint velocities is given by

$$\mathcal{V}_e = \mathcal{J}_e \dot{\theta} \quad (1)$$

where $\mathcal{J}_e \in \mathcal{R}^{6n_e \times \mathcal{N}}$ denotes the combined Jacobian matrix for all the end-effector nodes. \mathcal{J}_e is formed by a row-wise stacking of the individual $6 \times \mathcal{N}$ Jacobian matrices for each of the individual end-effector nodes.

Now consider known spatial forces $f_e \in \mathcal{R}^{6n_e}$ being applied to the system at the end-effector nodes. The joint space equations of motion for the tree-topology system are¹

$$\mathcal{M}(\theta)\ddot{\theta} + \mathcal{C}(\theta, \dot{\theta}) - \mathcal{J}_e^* f_e = \mathcal{T} \quad (2)$$

where the configuration dependent, symmetric matrix $\mathcal{M}(\theta) \in \mathcal{R}^{\mathcal{N} \times \mathcal{N}}$ is the *mass matrix* of the system, $\mathcal{C}(\theta, \dot{\theta}) \in \mathcal{R}^{\mathcal{N}}$ denotes the velocity dependent Coriolis and gyroscopic forces and gravitational forces vector, and $\mathcal{T} \in \mathcal{R}^{\mathcal{N}}$ denotes the applied joint torques. The mass matrix is positive-definite and invertible for tree-topology systems.

Instead of the joint space view, operational space dynamics characterizes the system dynamics as reflected to the end-effector nodes. It defines the relationship between f_e and the $\alpha_e \in \mathcal{R}^{6n_e}$ spatial accelerations of the end-effector nodes. Differentiating Eq. 1 with respect to time, we obtain

$$\alpha_e \stackrel{1}{=} \mathcal{J}_e \ddot{\theta} + \dot{\mathcal{J}}_e \dot{\theta} \quad (3)$$

Pre-multiplying both sides of Eq. 2 by $\mathcal{J}_e \mathcal{M}^{-1}$ and using Eq. 3 leads to

$$\alpha_e \stackrel{2,3}{=} \Gamma_e f_e + \mathcal{J}_e \mathcal{M}^{-1} (\mathcal{T} - \mathcal{C}) + \dot{\mathcal{J}}_e \dot{\theta} \quad (4)$$

where

$$\Gamma_e \triangleq \mathcal{J}_e \mathcal{M}^{-1} \mathcal{J}_e^* \in \mathcal{R}^{6n_e \times 6n_e} \quad (5)$$

Eq. 4 defines the operational space dynamics for a tree topology system. Γ_e is referred to as the *operational space compliance matrix (OSCM)* for the end-effector nodes in the tree-topology system. Its inverse, when it exists, is referred to as the *operational space inertia matrix (OSIM)* for the end-effector nodes. The invertibility of Γ_e does not depend on \mathcal{J}_e being invertible — only that \mathcal{J}_e have full row-rank, or equivalently that the null-space of \mathcal{J}_e^* consist of just the trivial zero element. Γ_e is singular when this null space is non-trivial. All end-effector forces f_e belonging to the null-space are *squeeze* forces, in the sense that they only contribute to internal forces, and no motion, since they have no effect on the α_e end-effector spatial accelerations. The OSIM always exists for a free-floating system with a single end-effector node since it is simply the 6×6 articulated body inertia with the end-effector node's parent body serving as the base body [13].

Since our focus is on the OSCM, with no loss in generality we simplify the further discussion by assuming that the system is at rest and the joint torques and gravity are zero, i.e. $\dot{\theta} \equiv 0$ and $\mathcal{T} \equiv 0$. The velocity and torque dependent terms such as \mathcal{C} and $\dot{\mathcal{J}}_e$ become zero with this assumption.

3 Closed-Chain Systems

Closed-chain systems can be viewed as tree-topology systems subject to additional bilateral closure constraints on the system. Such closure constraints can be either *holonomic* or *non-holonomic*. In the velocity domain the constraint equations can be expressed as

$$G_c(\theta, t)\dot{\theta} = 0 \quad (6)$$

¹The A^* notation denotes the transpose of the A matrix.

with $G_c(\theta, t) \in \mathcal{R}^{n_c \times \mathcal{N}}$ denoting the constraint matrix. Since we are focusing here on the OSCM, we assume without any loss in generality that $G_c(\theta, t)$ is time-invariant, i.e., $G_c(\theta, t) \equiv G_c(\theta)$. We assume that $G_c(\theta)$ is a *full-rank* matrix. A notable point about Eq. 6 is that it is linear in the generalized velocity coordinates. These constraints effectively reduce the generalized velocities for the system from an \mathcal{N} to an $(\mathcal{N} - n_c)$ dimensional linear space,

The dynamics of closed-chain systems can be obtained by modifying the tree system dynamics in Eq. 2 to include the effect of the closure constraints via *Lagrange multipliers*, $\lambda \in \mathcal{R}^{n_c}$, as follows

$$\begin{aligned} \mathcal{M}(\theta)\ddot{\theta} - \mathcal{J}_e^* f_e - G_c^*(\theta)\lambda &= 0 \\ G_c(\theta)\dot{\theta} &= 0 \end{aligned} \quad (7)$$

The $-G_c^*(\theta)\lambda$ term in the first equation represents the generalized forces arising from the presence of closure constraints. The following lemma describes a solution for the closed chain dynamics in Eq. 7.

Lemma 1 Closed-chain forward dynamics solution

The closed-chain dynamics generalized accelerations in Eq. 7 can be expressed as

$$\ddot{\theta} = \mathcal{M}^{-1} \left\{ I - G_c^* [G_c \mathcal{M}^{-1} G_c^*]^{-1} G_c \mathcal{M}^{-1} \right\} \mathcal{J}_e^* f_e \quad (8)$$

Proof: See [10, 13, 15].

4 Closed-chain OSCM

For tree topology systems, Eq. 4 and Eq. 5 define the operational space relationship between the f_e end-effector node spatial forces and their α_e spatial accelerations, and the expression for the associated Γ_e OSCM. We generalize this notion, and define a matrix $\Gamma \in \mathcal{R}^{6n_e \times 6n_e}$ as being the OSCM for a closed-chain system if it satisfies the analogous relationship

$$\alpha_e = \Gamma f_e \quad (9)$$

for the system. The following lemma provides an explicit expression for Γ .

Lemma 2 The OSCM with closure constraints

The OSCM for the end-effector nodes for a closed-chain system is given by

$$\Gamma = \Gamma_e - \mathcal{J}_e \mathcal{M}^{-1} G_c^* [G_c \mathcal{M}^{-1} G_c^*]^{-1} G_c \mathcal{M}^{-1} \mathcal{J}_e^* \quad (10)$$

which is the *Schur complement*² of the $G_c \mathcal{M}^{-1} G_c^*$ sub-block matrix in the matrix X defined as

$$X \triangleq \begin{bmatrix} \mathcal{J}_e \\ G_c \end{bmatrix} \mathcal{M}^{-1} \begin{bmatrix} \mathcal{J}_e^* & G_c^* \end{bmatrix} = \begin{pmatrix} \Gamma_e & \mathcal{J}_e \mathcal{M}^{-1} G_c^* \\ G_c \mathcal{M}^{-1} \mathcal{J}_e^* & G_c \mathcal{M}^{-1} G_c^* \end{pmatrix} \quad (11)$$

Proof: Multiplying both sides of Eq. 8 by \mathcal{J}_e and using the expression for the α_e end-effector spatial accelerations from Eq. 3 results in Eq. 9 with

$$\Gamma = \mathcal{J}_e \mathcal{M}^{-1} \left\{ I - G_c^* [G_c \mathcal{M}^{-1} G_c^*]^{-1} G_c \mathcal{M}^{-1} \right\} \mathcal{J}_e^* \quad (12)$$

Expanding out the right hand side and using Eq. 5 leads to Eq. 10.

Observe that the Eq. 10 expression for the Γ closed-chain OSCM depends on the Γ_e tree OSCM for the end-effector nodes. The expression in the second equation in Eq. 12 is also derived and used in [16]. This X matrix is also used in control schemes for managing both the end-effector and internal constraint forces [15].

The following lemma shows that Γ is always positive semi-definite and is less positive-definite than the Γ_e tree OSCM.

²For a square block matrix $Y = \begin{pmatrix} A & B \\ C & D \end{pmatrix}$ with invertible D , the *Schur complement* of D in Y is defined as the $A - BD^{-1}C$ matrix.

Lemma 3 Relationship between Γ and Γ_e

$$\Gamma_e \geq \Gamma \geq 0 \tag{13}$$

Proof: The $\Gamma_e \geq \Gamma$ relationship follows directly by using the fact that $\mathcal{J}_e \mathcal{M}^{-1} G_c^* [G_c \mathcal{M}^{-1} G_c^*]^{-1} G_c \mathcal{M}^{-1} \mathcal{J}_e^*$ is always positive semi-definite in Eq. 10.

To establish³ $\Gamma \geq 0$, define the matrix $P = G_c^* [G_c \mathcal{M}^{-1} G_c^*]^{-1} G_c \mathcal{M}^{-1}$ and observe that $P^2 = P$, implying that P is a projection matrix. Since P is a projection matrix, so is $P_\perp \triangleq I - P$. P_\perp is also referred to as the *mass-weighted constraint null space projection matrix* [15]. It is easy to verify that

$$\mathcal{M}^{-1} P = P^* \mathcal{M}^{-1} = P^* \mathcal{M}^{-1} P \text{ and } P^* \mathcal{M}^{-1} P_\perp = 0 \tag{14}$$

Using P , the expression for Γ in Eq. 12 can be restated as

$$\Gamma \stackrel{12}{=} \mathcal{J}_e \mathcal{M}^{-1} P_\perp \mathcal{J}_e^* \stackrel{14}{=} \mathcal{J}_e P_\perp^* \mathcal{M}^{-1} P_\perp \mathcal{J}_e^* \tag{15}$$

The positive semi-definiteness of Γ follows from this symmetric expression.

This lemma is in line with our intuitive expectation that the system with closure constraints should be at least as stiff, if not stiffer than the tree system alone without the closure constraints.

Γ needs to be positive definite for the corresponding OSIM, Γ^{-1} to exist. It is clear from Eq. 15 that Γ will be positive definite if and only if $\mathcal{J}_e P_\perp^*$ has full row rank. This can be expensive to verify given the complexity of evaluating P since the mass matrix inverse is required. The following lemma describes simpler conditions under which Γ is positive-definite and hence invertible.

Lemma 4 Positive definiteness of the Γ OSCM

Γ is positive definite if and only if $\begin{bmatrix} \mathcal{J}_e \\ G_c \end{bmatrix}$ has full row-rank.

Proof: Recall that Γ is the Schur complement of the X matrix in Eq. 11. From matrix theory, it is known that the Schur complement for a symmetric semi-definite matrix is positive definite if and only if the full matrix is positive definite [18]. Γ is therefore positive definite if and only if X is positive definite. Since \mathcal{M}^{-1} is always positive definite, X is positive definite if and only if $\begin{bmatrix} \mathcal{J}_e \\ G_c \end{bmatrix}$ has full row-rank, and the result follows.

This lemma establishes the conditions for the non-singularity of Γ . The full row-rank requirement on $\begin{bmatrix} \mathcal{J}_e \\ G_c \end{bmatrix}$ of course requires that \mathcal{J}_e itself have full row-rank and hence that the Γ_e tree OSCM itself be non-singular. Moreover, the full row-rank requirement on $\begin{bmatrix} \mathcal{J}_e \\ G_c \end{bmatrix}$ is equivalent to requiring that the null-space of $[\mathcal{J}_e^*, G_c^*]$ consist of only the zero element.

This is a generalization of the condition for tree-topology systems where a similar condition only applied to the null-space of \mathcal{J}_e^* . When the null-space of $[\mathcal{J}_e^*, G_c^*]$ is non-trivial, Γ is singular. Moreover, all elements of the null-space define the squeeze forces for the constrained system. To see this, let us assume that $\begin{bmatrix} x \\ y \end{bmatrix}$ is an element of the null-space, and therefore

$$\mathcal{J}_e^* x + G_c^* y = 0 \Rightarrow \mathcal{J}_e^* x = -G_c^* y$$

Using this x for f_e in Eq. 8 leads to $\ddot{\theta} = 0$. Hence $f_e = x$ is a squeeze end-effector force for the system since it does effect the system motion.

Clearly this sub-space of squeeze forces for the closed-chain system embeds the tree-system squeeze forces defined by the null-space of \mathcal{J}_e^* . That is, if z is a squeeze force for the tree system, then z must be in the null-space of \mathcal{J}_e^* , and therefore $\begin{bmatrix} z \\ 0 \end{bmatrix}$ is in the null-space of $[\mathcal{J}_e^*, G_c^*]$. As a consequence, the multi-link structure with closure constraints can resist a larger space of end-effector forces than just the tree system without the closure constraints.

³This proof is based on a reviewer’s suggestion and is simpler and more elegant than the original one proposed by the author.

5 Loop closure constraints

So far, we have not made any particular assumptions on the nature of, or the physical origin of, the closure constraints. In this section, we look at the important special case where the constraints are between body nodes in the tree-topology system. Such closure constraints between body nodes are referred to as *loop* constraints. An example is illustrated in Figure 1. Generally, these inter-node constraints are defined by hinges that allow non-zero relative spatial velocities that

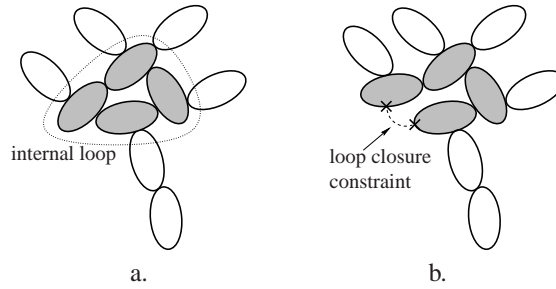


Figure 1. Example system with (a) closed-chain topology, and (b) after decomposing into a tree topology system with a loop closure constraint.

belong to a subspace defined by hinge joint map matrices. For instance, a loop closure constraint between a body node x and the inertial frame is characterized by an equation of the form

$$\mathcal{Q}\mathcal{V}_x = 0$$

where $\mathcal{V}_x \in \mathcal{R}^6$ is the spatial velocity of node x and $\mathcal{Q} \in \mathcal{R}^{\alpha \times 6}$ (with $\alpha \leq 6$), is the constraint matrix. A rigid constraint, where the node x is not allowed to move has an identity \mathcal{Q} matrix. On the other hand, a loop constraint on the relative spatial velocity of a pair of body nodes, x and y , can be expressed as

$$\mathcal{Q}^{\text{rel}} [\mathcal{V}_x - \mathcal{V}_y] = 0$$

This can be restated as

$$\mathcal{Q}\mathcal{V}_b = 0 \text{ where } \mathcal{Q} \triangleq [\mathcal{Q}^{\text{rel}}, -\mathcal{Q}^{\text{rel}}], \mathcal{V}_b \triangleq \begin{bmatrix} \mathcal{V}_x \\ \mathcal{V}_y \end{bmatrix} \quad (16)$$

When the x and y nodes are constrained to rigidly follow each other, the \mathcal{Q}^{rel} matrix is the identity matrix.

More generally, let us assume that there are n_b such loop *closure* body nodes with $\mathcal{V}_b \in \mathcal{R}^{6n_b}$ denoting the stacked vector of spatial velocities of these nodes. Let the closure constraints be defined on pairs of these nodal spatial velocities via a constraint matrix $\mathcal{Q} \in \mathcal{R}^{n_c \times 6n_b}$ such that

$$\mathcal{Q}\mathcal{V}_b = 0 \quad (17)$$

With $\mathcal{J}_b \in \mathcal{R}^{6n_b \times \mathcal{N}}$ denoting the velocity Jacobian matrix for these closure nodes we have

$$\mathcal{V}_b = \mathcal{J}_b \dot{\theta} \Rightarrow \mathcal{Q}\mathcal{J}_b \dot{\theta} \stackrel{17}{=} 0 \Rightarrow \mathcal{G}_c \stackrel{6}{=} \mathcal{Q}\mathcal{J}_b \quad (18)$$

From Eq. 7 it follows that the generalized forces from the Lagrange multipliers are given by

$$\mathcal{G}_c^*(\theta)\lambda = \mathcal{J}_b^* \mathbf{f}_b \text{ where } \mathbf{f}_b \triangleq \mathcal{Q}^* \lambda \quad (19)$$

\mathbf{f}_b is the stacked vector of constraint spatial forces at the loop-closure nodes arising from the loop closure constraints. Unlike the known \mathbf{f}_e end-effector forces, the \mathbf{f}_b loop closure forces on the system are *not available explicitly*, but are instead implicitly defined via the λ Lagrange multipliers. The following lemma provides an expression for the OSCM for the system with loop constraints.

Lemma 5 The OSCM with loop constraints

The OSCM for the end-effector nodes for the system with loop constraints is given by

$$\Gamma \triangleq \mathcal{J}_e \mathcal{M}^{-1} \left\{ \mathbf{I} - \mathcal{J}_b^* \mathcal{Q}^* [\mathcal{Q}\mathcal{J}_b \mathcal{M}^{-1} \mathcal{J}_b^* \mathcal{Q}^*]^{-1} \mathcal{Q}\mathcal{J}_b \mathcal{M}^{-1} \right\} \mathcal{J}_e^* \quad (20)$$

Proof: Eq. 20 results from substituting Eq. 18 into Eq. 10.

The Eq. 20 expression for Γ is complex and requires and involves the mass matrix inverse and the end-effector Jacobian matrices.

5.1 Relationship of Γ to a tree OSCM

We now develop an alternative expression for Γ that is based upon a tree OSCM. Towards this, define the full Jacobian, \mathcal{J}_f for the combined $n_f \triangleq n_e + n_b$ set of end-effector and closure nodes. \mathcal{J}_f maps the $\dot{\theta}$ generalized velocities to the $\mathcal{V}_f \in \mathcal{R}^{6n_f}$ spatial velocities of this full set of nodes. Thus

$$\mathcal{V}_f \triangleq \begin{bmatrix} \mathcal{V}_e \\ \mathcal{V}_b \end{bmatrix} = \mathcal{J}_f \dot{\theta} \Rightarrow \mathcal{J}_f \stackrel{1,18}{=} \begin{bmatrix} \mathcal{J}_e \\ \mathcal{J}_b \end{bmatrix} \in \mathcal{R}^{6n_f \times \mathcal{N}} \quad (21)$$

The Eq. 5 expression for tree OSCM can be extended to the tree OSCM for the combined set of end-effector and closure nodes $\Gamma_f \in \mathcal{R}^{6n_f \times 6n_f}$ using the \mathcal{J}_f full Jacobian as

$$\Gamma_f = \mathcal{J}_f \mathcal{M}^{-1} \mathcal{J}_f^* = \begin{pmatrix} \Gamma_e & \Gamma_{eb} \\ \Gamma_{eb}^* & \Gamma_b \end{pmatrix} \quad (22)$$

where

$$\begin{aligned} \Gamma_b &\triangleq \mathcal{J}_b \mathcal{M}^{-1} \mathcal{J}_b^* \in \mathcal{R}^{6n_b \times 6n_b} \\ \text{and } \Gamma_{eb} &\triangleq \mathcal{J}_e \mathcal{M}^{-1} \mathcal{J}_b^* \in \mathcal{R}^{6n_e \times 6n_b} \end{aligned} \quad (23)$$

Observe that Γ_f in Eq. 22 is defined in terms of the Γ_e tree OSCM for just the end-effector nodes and the Γ_b tree OSCM for just the closure nodes. The Γ_{eb} matrix represents the cross-coupling between the end-effector and closure nodes.

Lemma 6 Simpler expression for Γ with loop constraints

The OSCM for the end-effector nodes for the system with loop constraints is given by

$$\Gamma = \Gamma_e - \Gamma_{eb} \mathcal{Q}^* [\mathcal{Q} \Gamma_b \mathcal{Q}^*]^{-1} \mathcal{Q} \Gamma_{eb}^* \quad (24)$$

Proof: The result is obtained by substituting Eq. 23 into Eq. 20.

This alternate expression for the Γ OSCM with loop constraints is directly related to sub-blocks of the Γ_f tree OSCM. Γ is the Schur complement of Γ_e in the X matrix in Eq. 11, which we denote X_l for loop-constraints, and it has the simpler form

$$X_l = \begin{pmatrix} \Gamma_e & \Gamma_{eb} \mathcal{Q}^* \\ \mathcal{Q} \Gamma_{eb}^* & \mathcal{Q} \Gamma_b \mathcal{Q}^* \end{pmatrix} = \begin{pmatrix} \mathbf{I} & \mathbf{0} \\ \mathbf{0} & \mathcal{Q} \end{pmatrix} \Gamma_f \begin{pmatrix} \mathbf{I} & \mathbf{0} \\ \mathbf{0} & \mathcal{Q}^* \end{pmatrix} \quad (25)$$

We now discuss the significance of this and the earlier results in this paper:

- Unlike Eq. 20, the expression in Eq. 24 involves neither the mass matrix inverse nor the node Jacobians explicitly, and depends on the sub-blocks of the Γ_f tree OSCM. It clarifies the previously unknown, but intimate relationship between the closed-chain OSCM and an extended tree OSCM involving *both* the end-effector and the closure nodes. The Eq. 24 expression also separates the contributions of the closure nodes (through their OSCM sub-matrices) from that of the specific nature of the closure constraints (via the \mathcal{Q} matrix). When there are no closure constraint, \mathcal{Q} vanishes and Γ reduces to Γ_e .
- Important structural and analytical implications of Eq. 24 are that Γ does not require either the mass matrix inverse nor the Jacobians as implied by the earlier Eq. 12 expression. This observation is based on the spatial operator analysis that has established that the tree OSCM matrix [8, 10, 13] can be obtained directly from articulated body inertias without the need for the mass matrix inverse or the Jacobian. This applies to the Γ_f tree OSCM, and consequently via Eq. 24 also to the closed-chain Γ .

- The fact that Γ can be obtained from a tree OSCM also has important computational implications. the following two step procedure can be used to compute the closed chain Γ : (a) compute the Γ_f full tree OSCM using any available tree OSCM computational procedure; and (b) use the sub-blocks of Γ_f in Eq. 24 to evaluate Γ . This is significant because low-order techniques are available for computing tree OSCM matrices that can be used to efficiently carry out the first step. In particular, spatial operator recursive algorithms described in [10, 13] describe the lowest-order available algorithm for tree OSCM. An alternative sparsity-based algorithm for tree OSCM together with computational cost analysis can be found in reference [12]. Other recursive algorithms are described in references [9, 11]. It is noteworthy that the computational cost of these algorithms scales just linearly with the number of bodies.
- Loop-constraints are an important, but a special case of closure constraints. More generally, the closure constraints can consist of loop as well as non-loop constraints. We describe here the extensions to this more general case. To handle non-loop constraints, the G_c closure-constraint matrix in Eq. 18 can be extended to the following partitioned form

$$G_c = \begin{pmatrix} QJ_b \\ G_n \end{pmatrix} \quad (26)$$

where G_n corresponds to the non-loop closure constraints. Using this in Eq. 11 results in the following expression for the X matrix:

$$\begin{aligned} X &= \begin{pmatrix} \Gamma_e & \Gamma_{eb}Q^* & J_e G_n^* \\ Q\Gamma_{eb}^* & Q\Gamma_b Q^* & QJ_b^* M^{-1} G_n^* \\ G_n J_e^* & G_n M^{-1} J_b Q^* & G_n M^{-1} G_n^* \end{pmatrix} \\ &\stackrel{25}{=} \left(\begin{array}{c|c} X_l & \begin{bmatrix} J_e G_n^* \\ QJ_b^* M^{-1} G_n^* \end{bmatrix} \\ \hline [G_n J_e^*, G_n M^{-1} J_b^* Q^*] & G_n M^{-1} G_n^* \end{array} \right) \end{aligned} \quad (27)$$

From the second expression, it is clear that the loop-constraints X_l matrix from Eq. 25 is a sub-matrix of this overall X matrix, and our earlier observations about its OSCM based structure of X_l apply here as well. Denoting this lower block as Z

$$Z \triangleq \begin{pmatrix} Q\Gamma_b Q^* & QJ_b^* M^{-1} G_n^* \\ G_n M^{-1} J_b^* Q^* & G_n M^{-1} G_n^* \end{pmatrix} \quad (28)$$

the X matrix takes the form

$$X \stackrel{27,28}{=} \left(\begin{array}{c|c} \Gamma_e & [\Gamma_{eb}Q^*, J_e G_n^*] \\ \hline \begin{bmatrix} Q\Gamma_{eb}^* \\ G_n J_e^* \end{bmatrix} & Z \end{array} \right) \quad (29)$$

and thus using the Schur complement relationship from Lemma 2, Γ is given by

$$\Gamma = \Gamma_e - [\Gamma_{eb}Q^*, J_e G_n^*] Z^{-1} \begin{bmatrix} Q\Gamma_{eb}^* \\ G_n J_e^* \end{bmatrix} \quad (30)$$

This form allows us to takes full advantage of the tree OSCM techniques to compute X_l for the loop closure constraints. It also isolates the non-loop constraint blocks so they can be further analyzed and optimized once the specific form and structure of the non-loop constraints is available.

- While, much of our discussion has focused on the OSCM, Lemma 4, establishes the necessary condition for Γ to be non-singular and the closed-chain OSIM to exist.

6 Conclusions

This paper studies the OSIM and OSCM matrices for closed-chain topology robotic systems. The main contribution of this paper is to show that when closure constraints are loop constraints, the closed-chain OSCM is closely related, via a Schur complement, to the tree OSCM for the combined set of end-effector and closure nodes. This relationship has significant implications since it allows the application of the rich set of available analytical and computational implications for tree OSCM to closed-chain systems. We also discuss the positive definiteness properties of the closed-chain OSCM.

Acknowledgments

The research described in this paper was performed at the Jet Propulsion Laboratory (JPL), California Institute of Technology, under contract with the National Aeronautics and Space Administration⁴. This project was also supported in part by Grant Number RO1GM082896-01A2 from the National Institute of Health.

References

- [1] J. Nakanishi, R. Cory, Michael Mistry, J. Peters, and Stefan Schaal. Operational Space Control: A Theoretical and Empirical Comparison. *Internat. J. Robotics Res.*, 27(6):737–757, June 2008.
- [2] Bruno Siciliano and Oussama Khatib. *Springer Handbook of Robotics*. Springer, 2008.
- [3] Oussama Khatib. Object Manipulation in a Multi-Effector System. In *4th International Symposium on Robotics Research*, pages 137–144, Santa Cruz, CA, May 1988.
- [4] Oussama Khatib. A Unified Approach for Motion and Force Control of Robot Manipulators: The Operational Space Formulation. *IEEE Journal of Robotics and Automation*, RA-3(1):43–53, February 1987.
- [5] Oussama Khatib. The Operational Space Formulation in the Analysis, Design, and Control of Manipulators. In *3rd International Symposium Robotics Research*, Paris, 1985.
- [6] Oussama Khatib. Dynamic Control of Manipulators in Operational Space. In *6th CISM–IFTOMM Congress on Theory of Machines and Mechanisms*, New Delhi, India, December 1983.
- [7] K Kreutz-Delgado, Abhinandan Jain, and Guillermo Rodriguez. Recursive Formulation of Operational Space Control. In *3rd International Symposium on Robotics and Manufacturing*, Vancouver, Canada, June 1990.
- [8] K Kreutz-Delgado, Abhinandan Jain, and Guillermo Rodriguez. Recursive formulation of operational space control. *Internat. J. Robotics Res.*, 11(4):320–328, 1992.
- [9] K W Lilly and David E Orin. Efficient O(N) Computation of the Operational Space Mass Matrix. In *IEEE International Conference on Robotics and Automation*, Cincinnati, OH, May 1990.
- [10] Guillermo Rodriguez, Abhinandan Jain, and K Kreutz-Delgado. Spatial operator algebra for multibody system dynamics. *Journal of the Astronautical Sciences*, 40(1):27–50, 1992.
- [11] Kyong-sok Chang and Oussama Khatib. Efficient recursive algorithm for the operational space inertia matrix of branching mechanisms. *Advanced Robotics*, 4(8):703–715, 2001.
- [12] Roy Featherstone. Exploiting Sparsity in Operational-space Dynamics. *Internat. J. Robotics Res.*, 29(1992):1353–1368, September 2010.
- [13] Abhinandan Jain. *Robot and Multibody Dynamics: Analysis and Algorithms*. Springer, 2011.
- [14] Jeffrey Russakow, Oussama Khatib, and Stephen M Rock. Extended Operational Space Formulation for Serial-to-Chain (Branching) Manipulators. In *IEEE International Conference on Robotics and Automation*, number 1, pages 1056–1061, 1995.
- [15] Vincent De Sapio, Oussama Khatib, and Scott Delp. Task-level approaches for the control of constrained multibody systems. *Multibody System Dynamics*, 16(1):73–102, June 2006.
- [16] Jaeheung Park and Oussama Khatib. Contact Consistent Control Framework for Humanoid Robots. In *IEEE International Conference on Robotics and Automation*, number 1, pages 1963–1969, 2006.
- [17] Luis Sentis, Jaeheung Park, and Oussama Khatib. Compliant Control of Multicontact and Center-of-Mass Behaviors in Humanoid Robots. *IEEE T. Robot. Autom.*, 26(3):483–501, 2010.
- [18] S Boyd and L Vandenberghe. *Convex Optimization*. Cambridge University Press, 2004.
- [19] Nicolas Hudson, Thomas Howard, Jeremy Ma, Abhinandan Jain, Max Bajracharya, Steven Myint, Calvin Kuo, Larry Matthies, Paul G Backes, Paul Hebert, Thomas Fuchs, and J W Burdick. End-to-End Dexterous Manipulation with Deliberate Interactive Estimation. In *IEEE International Conference on Robotics and Automation*, Minneapolis, MN, 2012.

⁴©2013 California Institute of Technology. Government sponsorship acknowledged.